Test of correlation method to determine QUV↔QUV cross-talk

C. Beck

March 13, 2018

Contents

1 Introduction

The DKIST telescope will have a single calibration unit (CU) behind the second mirror (M2) for the polarimetric calibration of observations. The polarization properties of M1 and M2 can thus only be partly be measured using the CU, or more precisely, only the amount of linear polarization of the M12 group caused by the diattenuation X can be determined using the CU, not the mirror retardance τ. The currently proposed methods for the full determination of the M12 group parameters thus are: CU

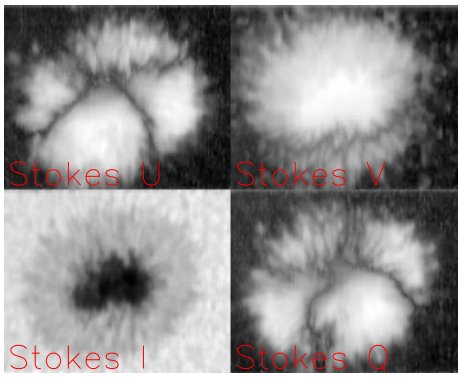

Figure 1: "Ideal" sunspot at 30 degrees heliocentric angle. Stokes Q and U show neutral lines every 90 degree in azimuth around the spot center that are offset by 45 degrees from each other. There is only one neutral line in Stokes V that is at a completely different location and that has a completely different orientation.

observations and I→QU cross-talk (X), correlation method for spectral lines without or with low intrinsic linear polarization (τ), sky polarization (X and τ) and correlation method of spectral lines with a regular Zeeman pattern, i.e., intrinsic QU and V signals (τ). The latter method suffers from the problem that in addition to the cross-talk between Stokes parameters all of QUV can show varying genuine polarization signals.

Two different approaches were proposed to disentangle the QUV↔QUV cross-talk from genuine polarization signals: assumptions on the symmetry properties of Stokes V (anti-symmetric) and Q or U (symmetric), or assumptions on the magnetic field geometry, i.e., in a sunspot, on the one hand, radial fields with a specific QU repetitive pattern are expected while, on the other hand, one location with zero QU should be present where the magnetic field is parallel to the line of sight.

2 Cross-talk determination using the correlation coefficient between $|QUV|$ maps

2.1 Rationale

One way to infer the polarization properties of a mirror system that has not been corrected for in the calibration is the determination of the (residual) cross-talk between polarization components. There are different ways how the correlation coefficient can be determined, e.g., using individual Stokes profiles or somehow averaged values. The determination of the cross-talk in individual profiles is based on the fact that the polarization signal in QU and V in a Zeeman-sensitive spectral line has an intrinsically different spectral shape (see Sect. 3 below). This method usually requires a pre-selection of the profiles to be used.

Another more robust and automatic method is the determination of the correlation coefficient between 2D maps of the wavelength-integrated unsigned polarization signal in Stokes QUV. The approach is based on the following assumptions:

- The residual cross-talk coefficient is wavelength-independent over a range of 1–2 nm.
- The spatial patterns of polarization signal in QUV are different.

The first point is ensured to first order by the amount of wavelength-dependent polarization properties that any type of optics can have. The only case of a strong-wavelength dependence in such a small wavelength range happens usually in slit-spectrograph instruments that have the polarizing beam splitters (BSs) close to the final spectral focal plane. The apparent wavelength-dependence in that case is, however, spurious, because it is in reality caused by the spatial variation of the polarizing properties of the BS. Since one of the spatial axes of the BS is along the dispersion direction, it creates the impression of a wavelength dependence, but that is not the case.

The second point of different spatial patterns in QUV is ensured by the magnetic field topology in the solar photosphere. All magnetic flux concentrations with a field strength above the equipartition field strength of about 400 G are pushed to a vertical orientation relative to the solar surface by buoyancy forces. They are also compressed in the horizontal dimension if they are in hydrostatic equilibrium with the surrounding field-free atmosphere volume. In the upper photosphere and the chromosphere, the

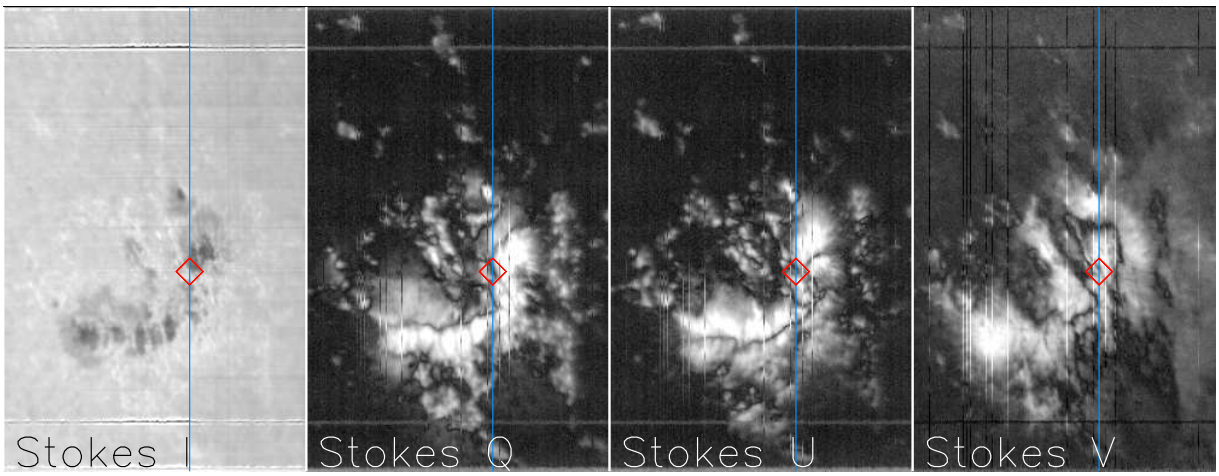

Figure 2: Overview maps of the scan at 851 nm used for the cross-talk determination. Left to right: Stokes I, wavelength-integrated unsigned QUV with the standard DST telescope correction. The blue vertical line indicates the location of the slit spectra shown in Fig. 3 and the red diamond the location of the profiles shown in Fig. 8.

magnetic pressure terms plus the internal gas pressure term start to be larger than the gas pressure of the external medium. This causes a lateral expansion of the flux concentration and creates increasingly more inclined magnetic field lines with increasing height. Since vertical magnetic fields create only Stokes V signals for a vertical line of sight (LOS), while horizontal field only create Q and U, the spatial pattern of any type of magnetic field concentration is a central maximum of the V signal that decreases with the radial distance, while Q and U have a minimum at center with an increase in the radial direction. The linear polarizations also show an azimuthal variation with iterative maxima and neutral lines, i.e., locations with zero polarization signal in a given Stokes parameter, every 90 degrees that is offset by 45 degrees between Q and U (see Fig. 1). Inclined LOSs and more complex magnetic topologies can modify that pattern, but the resulting spatial QUV pattern always predicts that Q, U and V do still differ from each other. An especially prominent pattern is created by the zero-crossings in QUV that for any roughly radial magnetic field topology cannot coincide all of the time (Fig. 2).

Another factor for the different spatial patterns in QU and V is the polarization amplitude. The circular polarization signal scales with the cosinus of the angle between the LOS and the magnetic field lines, while Q and U are proportional to sinus^2. The amplitudes of Q and U are thus usually lower than for V, to the point that in the magnetically quiet Sun nearly no linear polarization signal is seen. A pattern of co-spatial Q, U and V signals all over the field of view thus indicates cross-talk between polarization states rather than genuine solar polarization signal. These assumptions on the spatial variation and the value of the cross talk between Stokes V, and Q and U were confirmed using cross-talk-free spectra from magneto-hydrodynamic simulations (see Appendix 13.1).

For the determination of the residual cross-talk from the correlation of 2D maps of $|QUV|$, one map taken with the SPINOR instrument in the photospheric Fe I line at 851 nm was used. This line had been selected for the observations as being close to the standard chromospheric Ca II IR line at 854 nm. The initial calibrated data had a noise rms of $5{\cdot}10^{-4}$ in Stokes QU and $3{\cdot}10^{-3}$ in Stokes V. The difference is caused by the presence of interference fringes primarily in Stokes V (see Fig. 19 below). The integration time had been 12 s per scan step. The spectral sampling was about 6 pm per pixel giving a sampling-limited spectral resolution $R = \frac{\lambda}{\Delta\lambda} \approx 70,000$. The full dimensions of the scan were 252 steps with 386 pixel along the slit for a total of about 100,000 spectra. The observational target was an active region of a large heliocentric angle of 70 degrees.

The observational data was corrected with the standard polarimetric calibration pipeline of the SPINOR instrument that includes a correction for all telescope optics. Since it is, however, known, that the telescope calibration comes with some error, the data contains residual cross-talk at the percent level. That amplitude is comparable to the values that are predicted for the M12 group of DKIST with matrix

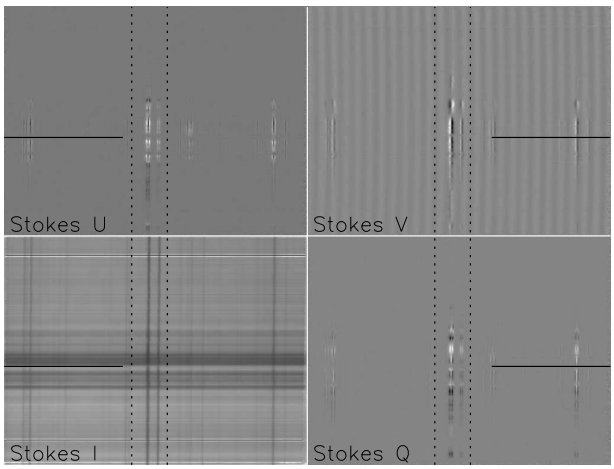

Figure 3: Slit spectra from the location marked in Fig. 2. The vertical dashed lines denote the wavelength region around the 851 nm line that was used in the integration and the horizontal black line the location of the profiles shown in Fig. 8.

elements of 0.1–8×10^{-2}. For the DKIST application, the actual application of the correction for the M12 group will be skipped to produce the cross-talk on purpose and to derive mirror properties from the cross-talk level. It is impossible to directly see the residual cross-talk contained in the slit-spectra in the case of these 851 nm data (Fig. 3), while in the plot of individual profiles in Fig. 7 below it shows up. Cross-talk is a second order effect, in which a polarization signal of a few ten percent is multiplies with a coefficient of percent level. Only cross-talk on the 10–20 % level is visible at once in a plot of spectra such as in Fig. 3.

2.2 Determination of residual V→QU cross-talk

The approach for the determination of the residual cross-talk between Stokes parameters was as follows. The original spectra were modified by, e.g., for the determination of V→QU cross-talk:

$$QU_{mod}(\alpha_{QU}) = QU_{orig} + \alpha_{QU} \cdot V\,, \tag{1}$$

where $\alpha_{QU} = -0.25...0.25$ in steps of about 0.017. For the $QU \rightarrow V$ cross-talk, the roles of QU and V in Eq. 1 were just exchanged.

For the original and modified spectra, maps of the unsigned wavelength-integrated polarization amplitude were constructed by running

$$|QUV|(x,y) = \int_{\lambda_0}^{\lambda_1} |QUV(x,y,\lambda)| d\lambda\,, \tag{2}$$

over all profiles $QUV(x,y,\lambda)$ where x, y indicates the location of one pixel inside the field of view.

The wavelength range λ_0 to λ_1 is indicated by the vertical dashed lines in Fig. 3. Note that for the creation of such maps it is not relevant if the spectral line enclosed has a regular Zeeman pattern, shows the Hanle effect or has no intrinsic linear polarization, as long as the line selected has any type of solar polarization signal that obeys the requirements in Sect. 2.1, i.e., different spatial - not spectral ! - patterns in QU and V. The original $|QUV|$ maps are shown in Fig. 2, while Fig. 4 shows maps of $|QU|_{mod}$ for different values of α_{QU}. The target region of these observations was quite off the disc center, so the Stokes V signals are comparably lower than for an active region near the center. The main effect of the artificial or additional cross-talk introduced into $|QU|_{mod}$ that can be seen in Fig. 4 thus is an increased level of diffuseness or the disappearance of the neutral lines in Q and U for $|\alpha_{QU}| > 0.1$.

The effect is displayed with higher visibility in Fig. 5 that shows the maps of $|QV_{mod}|$ at two levels of cross-talk and their difference. The locations of neutral lines in a Stokes parameter are naturally the places that are most sensitive to cross-talk from another Stokes parameter, since a) neutral lines in different Stokes parameters are not co-spatial and b) any amount of cross-talk at once removes the neutral line. Figure 5 clearly demonstrates that in the case of the present data, the impact of the cross-talk is largest in the neutral lines. For observations in more magnetically quiet regions with a predominant

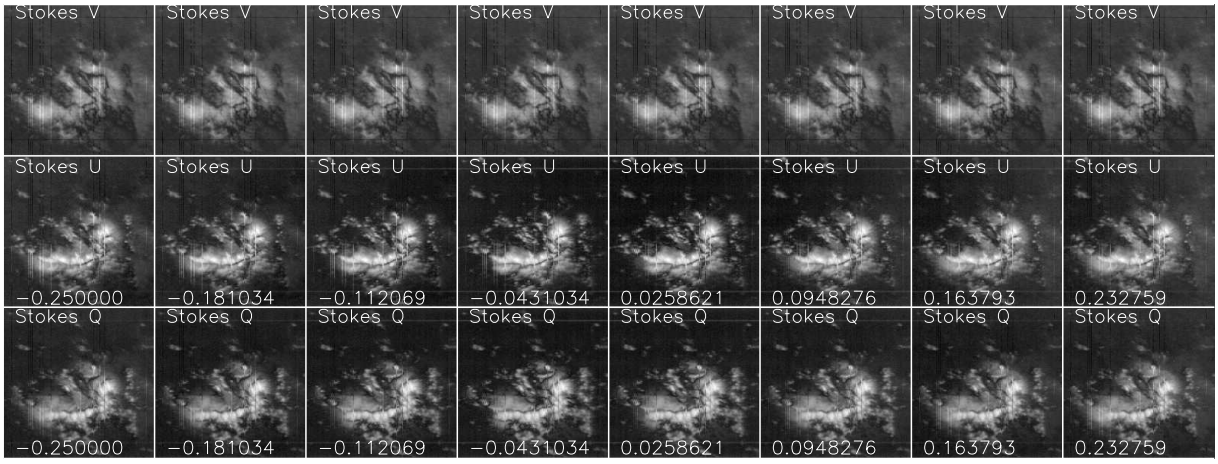

Figure 4: Maps of $|V|$ (top row) and $|Q|$ and $|U|$ at different values of the V→QU cross-talk applied. The cross-talk value is indicated at the bottom of the QU panels.

Stokes V signal, the cross-talk usually leads to spurious QU signals at every location with significant Stokes V signal instead of a zero QU amplitude, which is equivalent to a neutral line in Q or U.

The cross-talk between the maps of $|QUV|$ was then derived from the linear correlation coefficient that was calculated in a standard way by

$$C(|QU_{mod}|, |V_{orig}|, \alpha_{QU}) = \frac{S_1 \cdot S_2}{\sqrt{S_1^2 \cdot S_2^2}}\,, \tag{3}$$

where $S_1 = |QU_{mod}(\alpha_{QU})| - < |QU_{mod}(\alpha_{QU})| >$ and $S_2 = |V_{orig}| - < |V_{orig}| >$.

The advantage of the approach of using the wavelength-integrated maps and the linear correlation coefficient is that no assumptions on the spectral shape are required, only on the spatial distribution of the location of significant or non-zero polarization signal. Figure 6 shows the correlation coefficient for the $|QU_{mod}|$ and $|V_{orig}|$ maps of Fig. 2. The minimal correlation is reached at about -0.0240 for Stokes Q and 0.0026 for Stokes U. This values correspond to the expectation, because the data used were treated with the full polarimetric calibration so that only the error of the calibration should remain as residual cross-talk. The expected matrix entries for the M12 group of DKIST are of the same order.

2.3 Application of V→QU correction

With the determination of α_{QU} that leads to minimal correlation, the spectra of Q and U were corrected by

$$Q_{corr} = Q_{orig} - 0.0240 V_{orig} \quad \text{and} \tag{4}$$

$$U_{corr} = U_{orig} + 0.0026 V_{orig}\,. \tag{5}$$

Figure 7 shows slit-spectra of QUV before and after the correction. Similar to Fig. 3 neither the original cross-talk nor the improvement by the correction can be well seen. Only when selecting an individual profile that corresponds to a neutral line in Q or U (Fig. 8), the effect of the correction becomes visible, at least for Stokes Q. The profile shape of the line at 851 nm that is located at about the middle of the spectrum around pixel 250 changes from an anti-symmetric Stokes V shape with two lobes (2nd row from the top) to a symmetric regular Stokes Q shape with three lobes after the correction. The change in Stokes U is negligible, since a change by $0.0026 \cdot 0.04 = 0.0001 = 1 \cdot 10^{-4}$ cannot be detected visually.

2.4 Determination and correction for QU→V

The application of the same procedure on the $QU \rightarrow V$ cross-talk yielded values of $Q \rightarrow V = 0.0431$ and $U \rightarrow V = -0.0948$ (Fig. 9). The plot of the corrected V profiles in Fig. 10 shows a generic problem for the

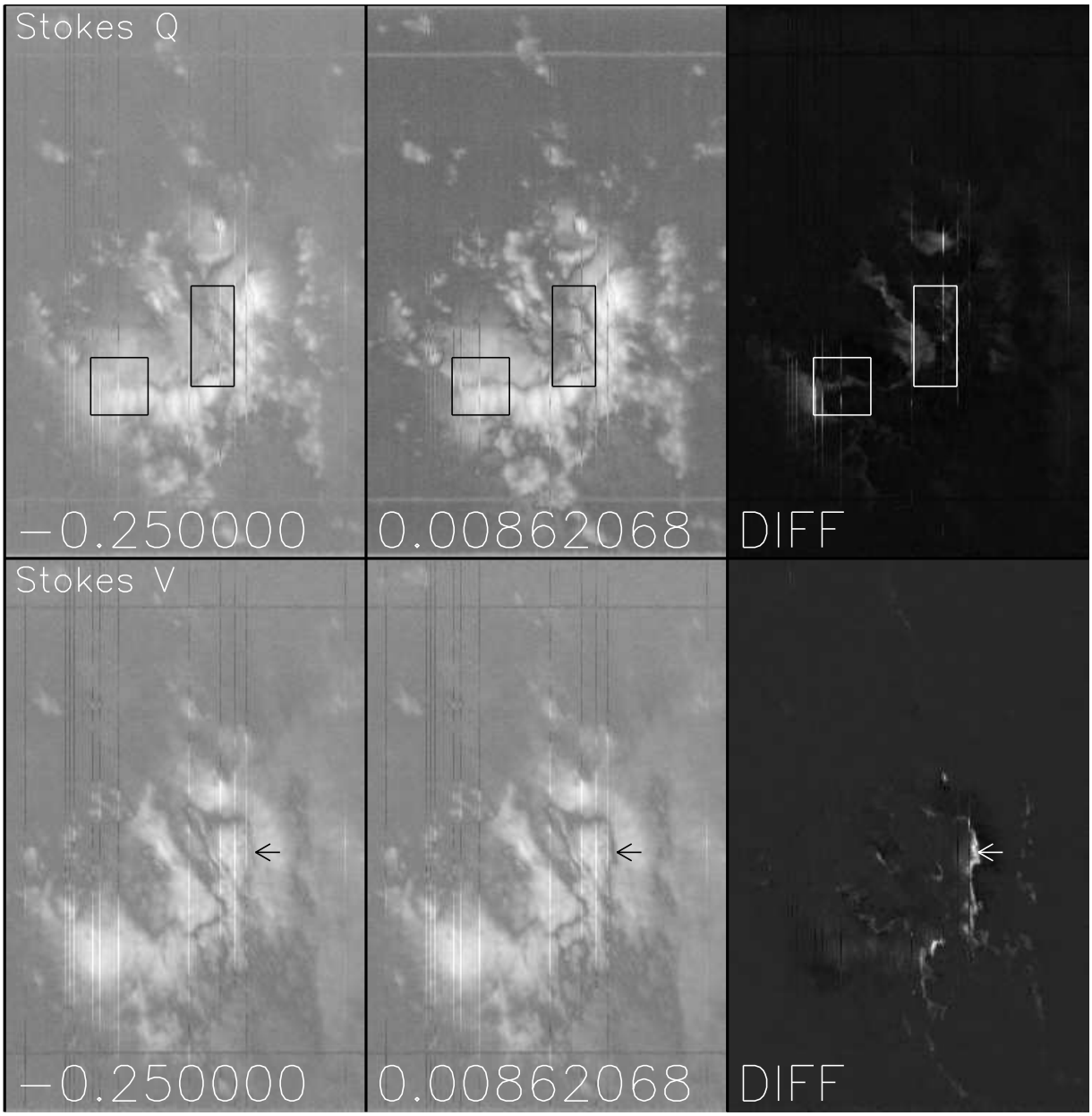

Figure 5: Maps of $|Q|$ (top) and $|V|$ (bottom) at two different levels of the V→Q and Q→V cross-talk applied. The right column shows the difference between the two maps at left to highlight the locations of the most significant changes that are indicated by arrows and rectangles.

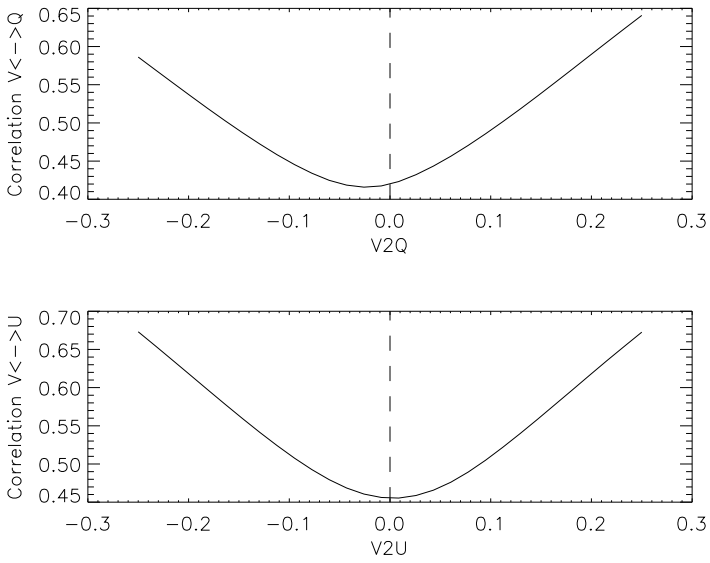

Figure 6: Correlation coefficient between maps of $|V|$ and $|Q|$ (top) and $|U|$ as a function of the V→QU cross-talk applied. The vertical dashed lines indicate zero cross-talk. The minimal correlation is reached at -0.0240 (Stokes Q) and 0.0026 (Stokes U).

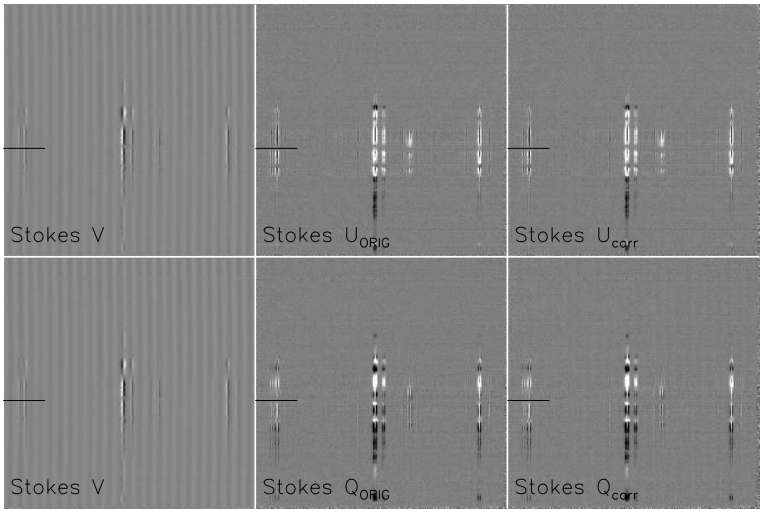

Figure 7: Slit spectra of Stokes V, Q and U from the location marked in Fig. 2 before and after the cross-talk correction. Left to right: Stokes V, original Stokes QU, and corrected Stokes QU. The horizontal black line indicates the location of the profiles shown in Fig. 8.

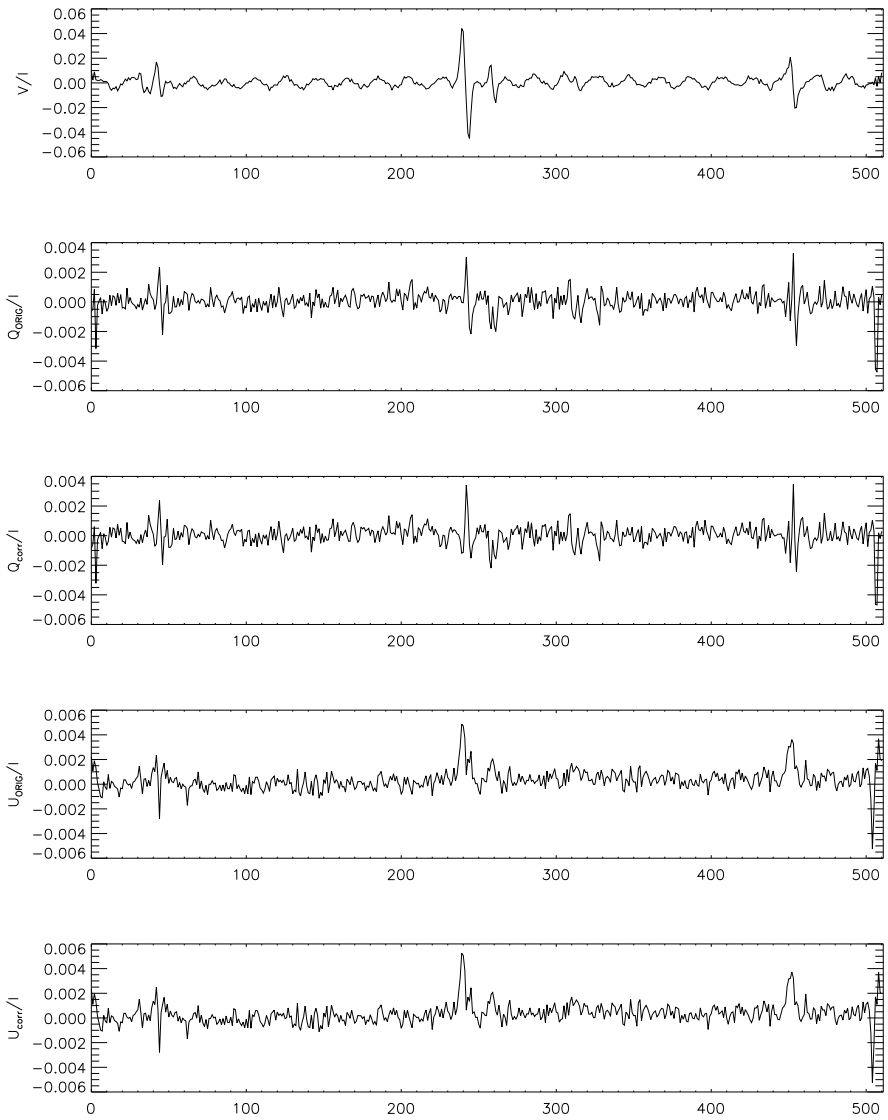

Figure 8: Profiles of Stokes Q and U from the location marked in Fig. 7 before and after the cross-talk correction. Top to bottom: Stokes V, original Stokes Q, corrected Stokes Q, original Stokes U and corrected Stokes U profile.

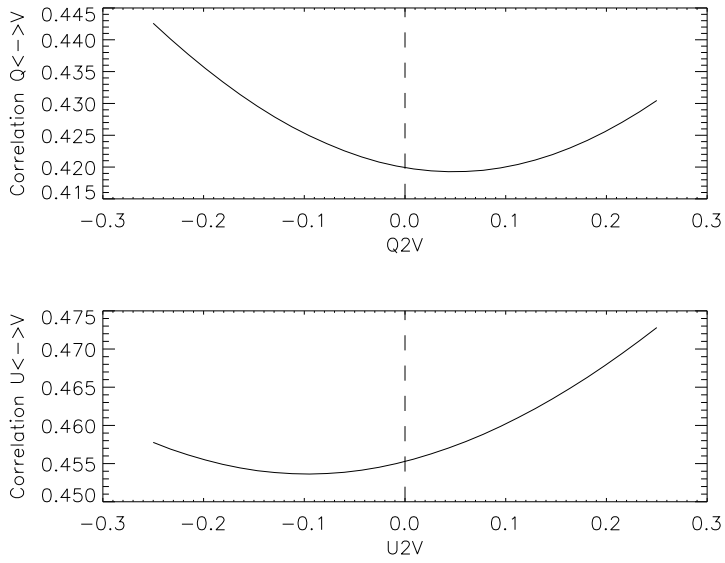

Figure 9: Correlation coefficient between maps of $|Q|$ and $|V|$ (top) and $|U|$ and $|V|$ as a function of the QU→V cross-talk applied. The vertical dashed lines indicate zero cross-talk. The minimal correlation is reached at 0.0431 (Stokes Q) and -0.0948 (Stokes U).

Table 1: $V \rightarrow QU$ cross-talk from the measurement and prior knowledge.

	α_{total}	α_{known}	$\alpha_{initial}$	$\alpha_{known} + \alpha_{initial}$	$\alpha_{total} - \alpha_{initial}$
Q	0.1604	0.1365	0.0240	0.1605	0.1364
U	0.0758	0.0732	0.0026	0.0758	0.0732

determination of cross-talk in that direction. The spectral shape of Stokes V (anti-symmetric) is different from both Q and U, but the latter have the same shape with not even necessarily an opposite sign. Any cross-talk value $Q \rightarrow V$ thus corresponds to some $U \rightarrow V$ coefficient, and the correction to Stokes V can be done using either the Q or U spectra. For the determination of the M12 group of DKIST, a parameter of the mirror group will be determined that matches primarily the $V \rightarrow QU$ cross-talk. The application of the M12 correction then should automatically minimize the $QU \rightarrow V$ cross-talk at the same time since the corresponding matrix entries are not independent, but connected through the parameter value.

2.5 Test on known cross-talk values

The test up to now was done on observational data with an unknown amount of residual cross-talk. The determination of the coefficients and the application of the correction improve the spectra (Fig. 8), but no definite statement on the accuracy of the determination can be made. We thus in addition introduced a known cross-talk between V and QU of 0.1365 and -0.0732 before the determination. Figure 11 and Table 1 show that these values are correctly retrieved.

The existence of cross-talk and the application of a correction on the 10^{-1} level now also has a clear visual impact on the spectra (Fig. 12). The uncorrected cross-talk leads to a clearly anti-symmetric profile shape in both Q and U which gets remedied by the correction.

Figure 13 shows a second method to visualize the quality of the cross-talk correction and a potential way of verifying cross-talk values. Given the presence of Stokes V signal over extended areas, the presence of, e.g., $V \rightarrow Q$ cross-talk increases the $|Q|$ value wherever $|V|$ is non-zero. In Fig. 13 it can be clearly seen that $|Q|$ reaches a minimum at locations without significant Q for the application of $V \rightarrow Q$ cross-talk between -0.164 and -0.147, i.e., flanking the exact value of 0.160. That approach to first order corresponds to determining the minimal in neutral lines of Q and U as a function of the $V \rightarrow QU$ cross-talk applied.

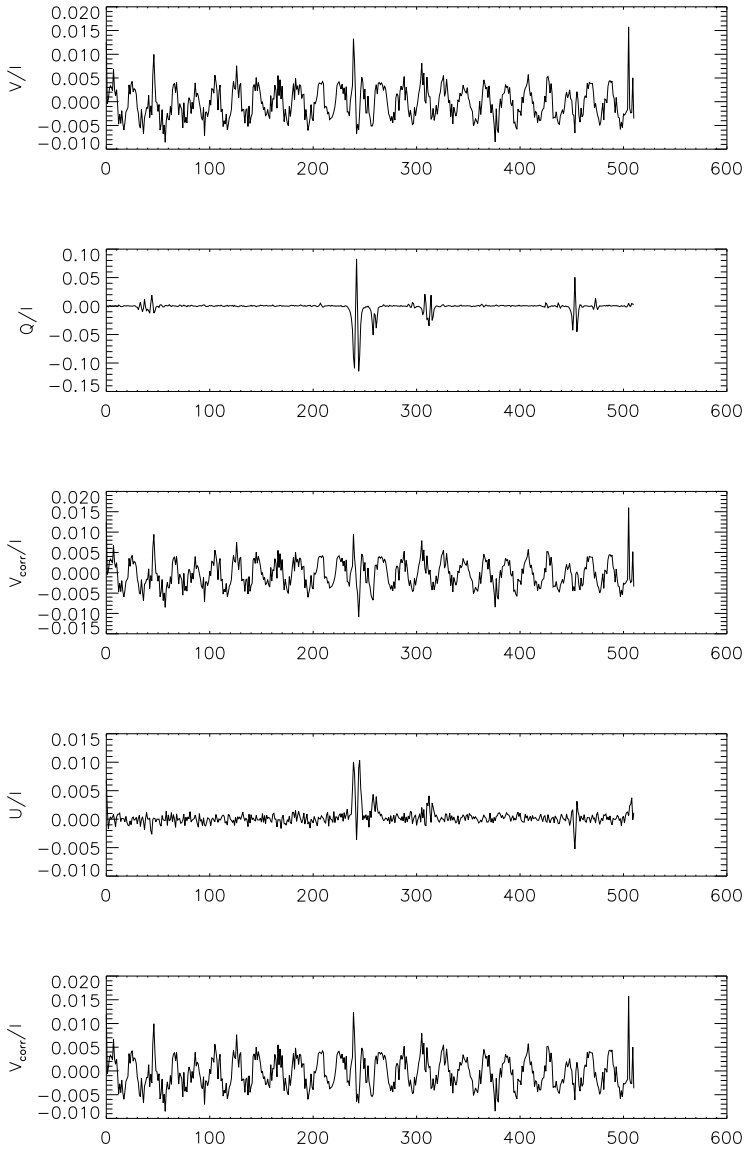

Figure 10: Profiles of Stokes V before and after the cross-talk correction. Top to bottom: original Stokes V, original Stokes Q, corrected Stokes V, original Stokes U and corrected Stokes V profile.

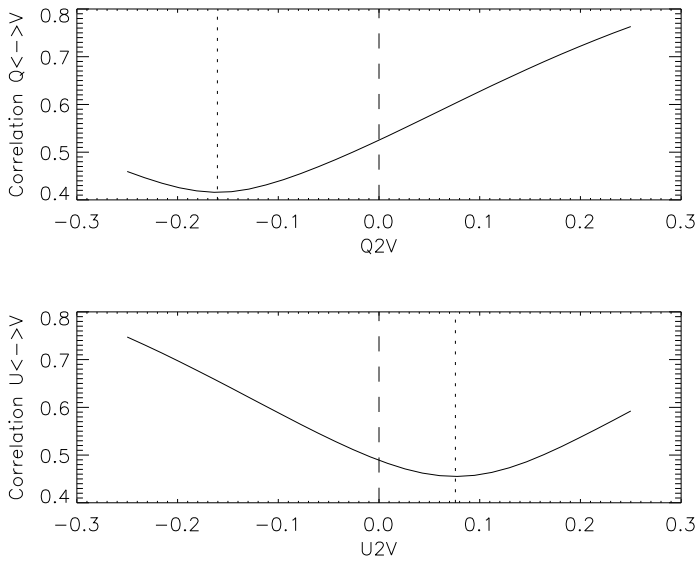

Figure 11: Correlation coefficient between maps of $|V|$ and $|Q|$ (top) and $|U|$ as a function of the V→QU cross-talk applied. The vertical dashed lines indicate zero cross-talk. The minimal correlation is reached at -0.1604 (Stokes Q) and 0.0758 (Stokes U).

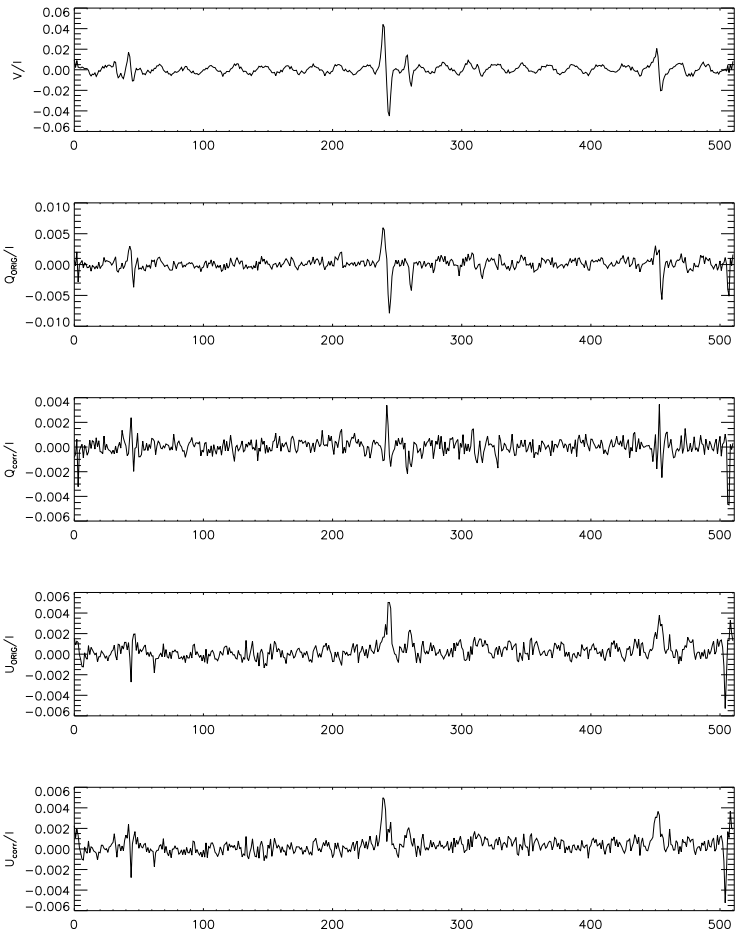

Figure 12: Profiles of Stokes Q and U from the location marked in Fig. 7 before and after the cross-talk correction. Top to bottom: Stokes V, artificial Stokes Q, corrected Stokes Q, artificial Stokes U and corrected Stokes U profile.

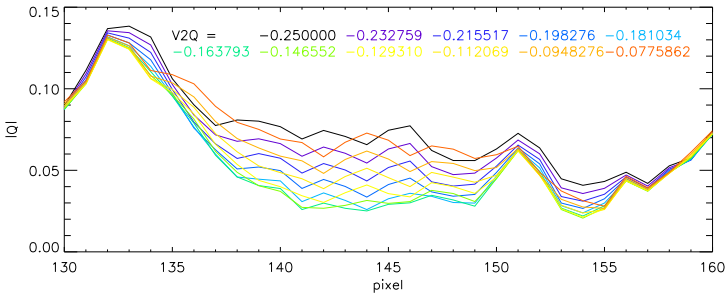

Figure 13: Spatial cut through the $|Q|$ map at step 140 for different values of the V→Q cross-talk applied.

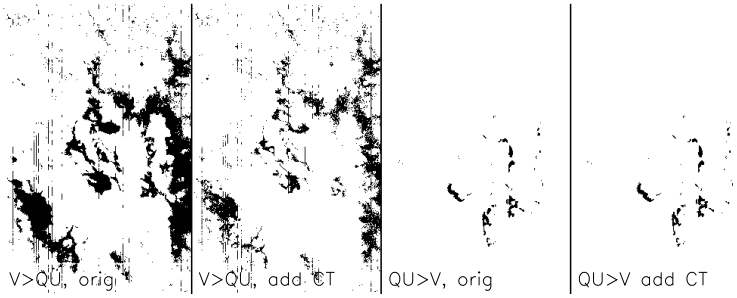

Figure 14: Left to right: spatial masks of locations with $|V| > 5 \cdot |QU|$ without and with additional cross-talk; the same for $|QU| > 2 \cdot |V|$.

3 Cross-talk determination using selected QUV profiles (Schlichenmaier/Collados)

Another method for the determination of residual $QUV \leftrightarrow QUV$ cross-talk is described in Schlichenmaier & Collados (2002, A&A, 381, 668). It is based on a pre-selection of the profiles to be used for the cross-talk determination.

3.1 Selection criterion

The selection criterion for using a profile for the $V \rightarrow QU$ cross-talk determination is that the amplitude $|V|$ in a profile is 5 times larger than both $|Q|$ and $|U|$. In the original paper, the same criterion was also used in the other direction, $|QU| > 5|V|$, but for the current data set, that did not leave a sufficient number of profiles. For $QU \rightarrow V$, a threshold of only twice the amplitude was used. Applying the selection criteria to the original data or those with the additional known cross-talk, led to the spatial masks shown in Fig. 14. From the total of about 100,000 profiles, only about 10,000 had $|V| > 5 \cdot |QU|$ and about 800 had $|QU| > 2 \cdot |V|$.

3.2 Determination of cross-talk

Using the masks as given above, the cross-talk is then determined by the fit of a linear coefficient to all profiles within the mask in one go by

$$QU = \alpha_{QU} \cdot V \,, \tag{6}$$

where either the original spectra or those with the added known cross-talk were used.

The results for this method are listed in Table 2. The $QU \rightarrow V$ cross-talk came out as 0.022 and −0.014, respectively. The known cross-talk values were retrieved with slightly lower accuracy in that case, with an error of the $1 - 4 \cdot 10^{-3}$ level. That might be due to the fact that for this method the spectral shape of the profiles is explicitly considered, because the determination of α_{QU} is based on it, which makes the approach more sensitive to the presence of interference fringes that are shared on QU and V.

Table 2: $V \rightarrow QU$ cross-talk from the measurement and prior knowledge.

	α_{total}	α_{known}	$\alpha_{initial}$	$\alpha_{known} + \alpha_{initial}$	$\alpha_{total} - \alpha_{initial}$
Q	0.1562	0.1365	0.0210	0.1575	0.1352
U	0.0721	0.0732	-0.0007	0.0725	0.0728

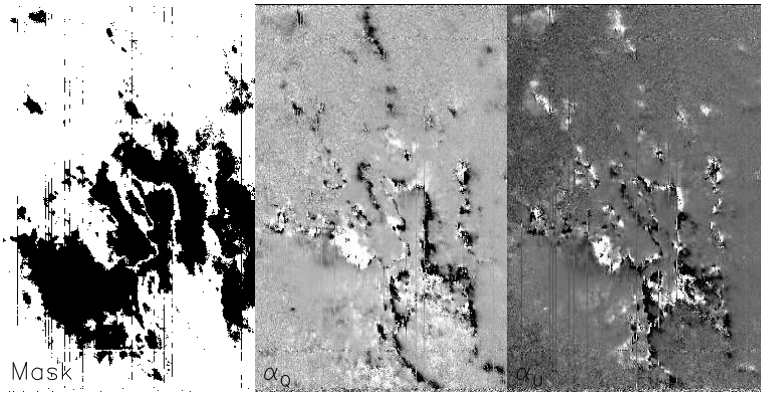

Figure 15: Left: mask of significant polarization signal in V/I > 0.015 with additionally $|V \rightarrow QU| < 0.5$. Middle/right: cross-talk coefficient $V \rightarrow QU$ as determined from the individual Stokes profiles after projection onto an anti-symmetric profile. The display range is ±0.4.

4 Cross-talk determination using symmetry properties (Elmore)

A third method for the determination of the cross-talk is based on making use of the expected spectral symmetry properties of the different Stokes parameters prior to applying a correlation measurement.

4.1 Symmetry assumptions & Data Preparation

The assumption for this method is that Stokes V is intrinsically anti-symmetric on almost all places on the solar surface, so any cross-talk from it should also still be anti-symmetric. The anti-symmetric part of the Stokes Q and U signal is isolated through a generic anti-symmetric function. To that extent, first all line-of-sight Doppler shifts are removed from the data using the line-core position of the spectral line to be used in Stokes I. Then the derivative with wavelength of each Stokes I profile is calculated, and the resulting derivatives are averaged. This provides an anti-symmetric Stokes-V-like curve that is centred at the common zero wavelength of all IQUV spectra after removal of the LOS velocities.

4.2 Determination of cross-talk

To determine the cross-talk, all QUV profiles are projected onto the averaged I derivative by simply multiplying with it. A scatter plot of the projected V vs. Q and U values in an individual profile then has to give a straight line whose slope is the cross-talk coefficient. In the presence of independent noise in Q, U and V, this is, however, not that straightforward anymore. To reduce the effect of noise on the determination, the spectra were first treated with a weak smoothing over 3 pixels before calculating a linear regression line to each individual set of projected QUV profiles.

The resulting spatial maps of α_{QU} are shown in the two right panels of Figure 15. Even with the noise filter and the usage of a regression line that corresponds to a linear fit, there was a significant scatter of the values. To improve the significance, a spatial mask based on the Stokes V amplitude (> 0.015) and a "reasonable" α_{QU} value (< 0.2; exact value is not very critical) was applied to select only pixels that meet both conditions.

Figure 16 shows the histograms of the resulting α_{QU} values across the FOV. Despite a still considerable scatter, the median (or even mean) values are well-defined. Table 3 lists the results for this method for

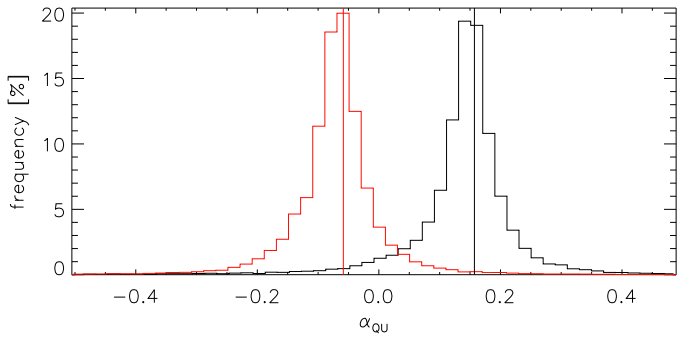

Figure 16: Histograms of α_Q (black) and α_U (red) for spectra with added known cross-talk. The vertical lines indicate the median values of 0.1572 and -0.0584, respectively.

Table 3: $V \rightarrow QU$ cross-talk from the measurement and prior knowledge.

	α_{total}	α_{known}	$\alpha_{initial}$	$\alpha_{known} + \alpha_{initial}$	$\alpha_{total} - \alpha_{initial}$
Q	0.1572	0.1365	0.0209	0.1574	0.1363
U	0.0584	0.0732	-0.0148	0.0584	0.0732

the initial spectra and after the addition of the known cross-talk values. The method retrieves the known offsets very well.

5 Summary: Methods

Table 4 summarizes the results from the different methods. As far as the unknown initial residual cross-talk is concerned, all three methods agree on a value of α_Q of 2.1–2.4 %. The scatter between the methods for α_U is much larger with values from -0.015 to $+0.0026$. When introducing additional known cross-talk, the method that uses selected QUV profiles performs worse than the other two, but that most likely results from the worse statistics for this approach.

From the point of computational effort, the last method needs slightly more computation steps and thus time, but still requires less than 10 s for a 100,000 profile map.

6 Second-order approach

One caveat about the current estimates is that the data was treated as having

$$V_{obs} \equiv V_{true} \tag{7}$$
$$Q_{obs} = Q_{true} + \alpha_Q V_{true} \tag{8}$$
$$U_{obs} = U_{true} + \alpha_U V_{true}\,, \tag{9}$$

Table 4: Measured initial $V \rightarrow QU$ cross-talk and average deviation when using known values.

Method	α_Q	α_U	Average error for known values
2D maps	0.0240	0.0026	$0.5 \cdot 10^{-4}$
Selected profiles	0.0210	-0.0007	$8 \cdot 10^{-4}$
Symmetry assumptions	0.0209	-0.0148	$1 \cdot 10^{-4}$

which is not the case. In reality

$$V_{obs} = V_{true} - \alpha_Q V_{true} - \alpha_U V_{true} + \alpha_{Q\to V} Q_{true} + \alpha_{U\to V} U_{true} \quad (10)$$
$$Q_{obs} = Q_{true} - \alpha_{Q\to V} Q_{true} - \alpha_{Q\to U} Q_{true} + \alpha_Q V_{true} + \alpha_{U\to Q} U_{true} \quad (11)$$
$$U_{obs} = ... \quad (12)$$

holds, where in principle all α_{ij} are independent of each other.

For all calculations up to now, the full set of equations is not critical because all next-order terms will go with $\alpha_{ij} \cdot \alpha_{kl} = O(\alpha^2)$. Given the fact that already terms like $\alpha_{ij} QUV_{obs}$ are difficult to detect in some cases because $|QUV| < 0.3$, any terms going with $\alpha_{ij}^2 QUV_{obs}$ can be well neglected.

For the application for the determination of M12 group properties of DKIST, the approach will be even less sensitive to the second-order terms. Instead of determining or varying specific cross-talk values between individual Stokes parameters, a parameter set that describes the complete Mueller matrix that contains all α_{ij} will be modified. In that case, hitting the "correct" solution will automatically solve Eqs. 10–12 in the sense that all $\alpha_{ij} \equiv 0$ so that $QUV_{obs} \equiv QUV_{true}$, with the caveats that a) any residual cross-talk only comes from the M12 group and b) that the description of the M12 group by the selected Mueller matrix and parameters is correct.

7 Discussion: Methods

The data set picked for the current study was randomly selected both in wavelength and in the target region. The latter actually is sort of the worst case, because it is a complex active region at a heliocentric angle of about 70 degrees where Stokes V is of the same order as Q and U instead of being significantly larger at most places. The have not been corrected for interference fringes before the evaluation. Still, all three methods were able to derive additional, known and significantly large cross-talk values with a high precision.

The fact that there is no good agreement on the initial residual cross-talk for Stokes U highlights one of the general problems in the determination of cross-talk. It is much easier and much more reliable to determine large cross-talk values than those close to zero. That is similar to the removal of fringes, where a large fringe amplitude makes the determination of the period and phase much easier than a fringe amplitude at the noise level. The prediction for $V \to U$ cross-talk for the M12 group is luckily on the order of 2–8 %, which should help in the correct determination of the mirror retardance.

In total, the method using explicitly selected QUV profiles seems to perform worst, presumably because it reduces the statistics too much. The usage of the projected QUV leads to a large scatter because of the large variation in the intrinsic profile shape. Both of these methods depend on the spectral shape of individual QUV profiles. The method that is based on wavelength-integrated quantities is more robust than the others against the profile shape or interference fringes because it only considers a spectrally average correlation. All of the methods will run into problems if there is any additional spatial variation of the cross-talk. All of them can be run on sub-fields on the FOV, but at the cost of reduced statistics.

8 Conclusion: Methods

From the current test on a randomly selected data set, an implementation of the method based on wavelength-integrated unsigned polarization amplitudes seems to work best. This approach is least affected by noise and interference fringes in the input spectra.

9 Additional tests

To expand the determination of accuracy, the method using wavelength-integrated unsigned polarization signals was tested under a variety of different additional degradations.

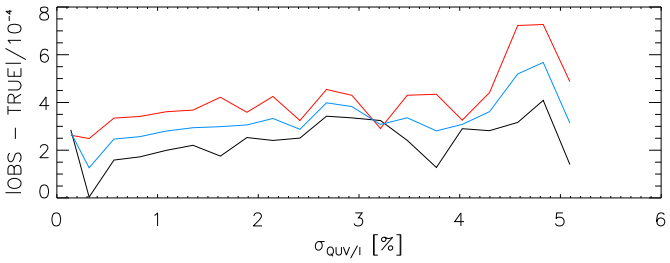

Figure 17: Average difference between derived and known added cross-talk for V→QU for increasing noise level.

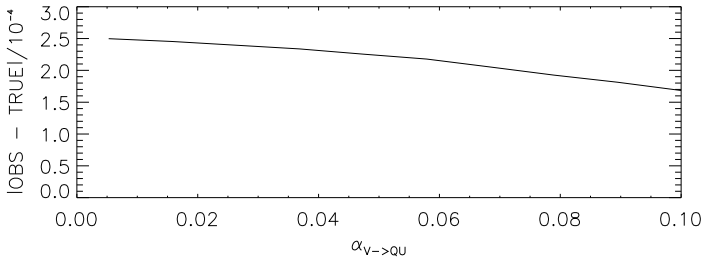

Figure 18: Average difference between derived and known added cross-talk for V→QU for increasing cross-talk amplitude.

9.1 Noise

To determine the dependence of the accuracy on the noise level in the data, all QUV spectra were added additional white noise of increasing rms amplitude after the introduction of a known V→QU cross-talk of 0.02. The rms noise level was varied from zero to 5 % QUV/I. Figure 17 shows that the uncorrelated noise increases the deviation between known and measured cross-talk by a factor of up to 4 at 5 % noise, but it is expected that that data used for the inference of M12 group parameters will have an rms noise of 1 % or less. The accuracy for any reasonable level of noise was about $4{\cdot}10^{-4}$.

9.2 Cross-talk amplitude

Figure 18 shows the difference between the known and derived V→QU cross-talk as a function of the cross-talk amplitude. The accuracy increases by a factor of about 2 from 0.01 to 0.1 cross-talk but again stayed at less than $2.5{\cdot}10^{-4}$ all the time.

9.3 Fringe amplitude

To test the sensitivity of the derivation against the fringe amplitude, three different data sets were used. One was corrected for fringes, one was the regular output of the data reduction without fringe correction, and one had the fringe amplitude in QUV increased by a factor of 4 before the introduction of the additional known V→QU cross-talk. It turned out that the accuracy in the determination did not react to the fringes and stayed at about 1–$4{\cdot}10^{-4}$ all the time. Figure 19 shows the most likely reason for that. The fringe amplitude in Stokes V is much larger than in Q and U, so the introduction of the additional known cross-talk was just creating a fringe pattern in Q and U that was proportional to the fringes in Stokes V. This test would best be repeated with synthetic data without fringes so that uncorrelated fringes in QUV could be introduced after the creation of the V→QU cross-talk.

9.4 Spatial variation and sub-fields

The current tests were done on data with some initial residual cross-talk. The additional cross-talk is introduced as a global factor that is constant across the field of view. This corresponds to cross talk from the M12 group at DKIST which is upstream of all other optics and is expected to show a minor field dependence. For the current data, there is, however, a potential mixture of “global” and “local”

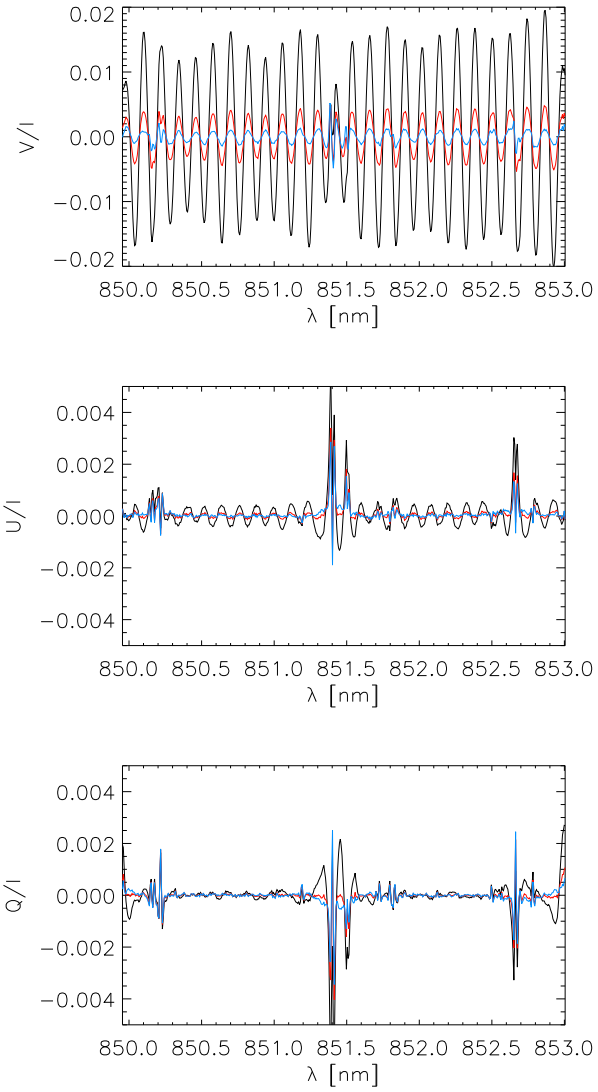

Figure 19: Stokes QUV (bottom to top) for three different fringe amplitudes at a constant added cross-talk value of V→QU = 0.02. Black: fringes increased by a factor of 4. Red: regular data reduction w/o fringe correction. Blue: fringe-corrected data.

cross talk if the actual polarization calibration of the data has left spatially varying cross-talk before the introduction of the additional constant cross talk.

To test both the spatial variation of the initial cross talk and the recovery of known additional cross talk with spatial resolution, the field of the view of the observations was split into 20 sub-fields of 12 columns each. The original Stokes V signals (left panel of Fig. 20) show a clear variation of the area coverage of significant polarization signal in each sub-field which naturally affects the statistics in each of them. The determination of the initial residual V→QU cross talk therefore shows a significant amount of variation in the spatial dimension. The average value was -0.02 ± 0.01 for Stokes Q and -0.0017 ± 0.029 in Stokes U, i.e., the standard deviation of the values is on the order of 10^{-2} and can be of the same order or even be much larger than the actual cross-talk value itself. In the case of the single map used for the current test, even the median and mean values over the 20 sub-fields differ by up to 0.01.

The difference between true and determined additional cross-talk stays at the order of 10^{-4} as for all other tests (Fig. 21), but only if the spatially varying initial cross talk is subtracted before, not its average or median value.

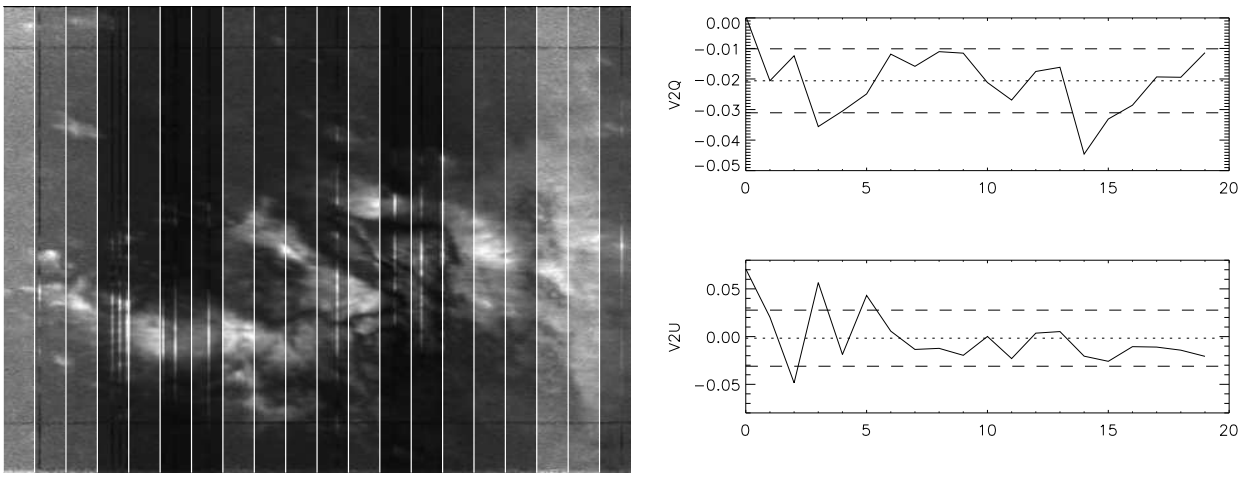

Figure 20: Left: wavelength-integrated unsigned Stokes V signal with vertical markers for the 20 sub-fields. Right: initial residual V→Q (top right) and V→U (bottom right) cross-talk in each sub-field. The dotted lines indicate the average value and the dashed line the rms fluctuation across the sub-fields.

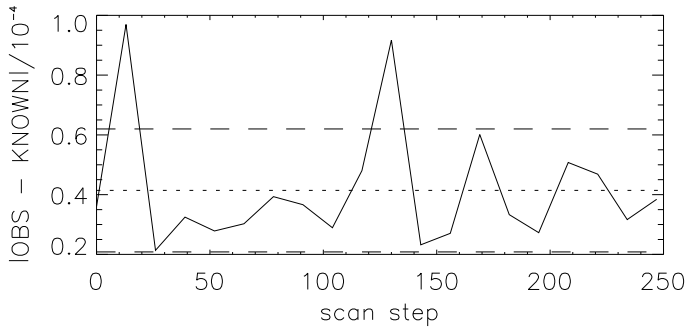

Figure 21: Average difference between derived and known added cross-talk for V→QU for the 20 sub-fields of 12 columns width each. The dotted line indicates the average value and the dashed line the rms fluctuation.

9.5 Different data set

To test the method on a second data set, a plage observation close to disc center at a heliocentric angle of 4 degrees was selected (see Fig. 22). The noise rms was similar to before with $3{\cdot}10^{-3}$ in Stokes V/I and $5{\cdot}10^{-4}$ in QU/I. The integration time was 16 s. The data clearly show a much larger residual cross talk. A first order guess by trial and error was -0.1 for V→Q and +0.1 for V→U. The field of view was cut to 252 x 331 pixels with a total of 80,000 profile to skip some rows at the top edge of the CCD that were not illuminated during the observations.

The maps of the wavelength-integrated unsigned Stokes $|QUV|$ at different cross talk levels in Figure 23 in this case show much more prominently the effect of the uncorrected or additional cross talk. For the extreme cross-talk values of ±0.3, Q and U resemble Stokes V, while there is a range in between where the spatial patterns are different.

The test of the spatial variation of the V→QU cross talk was done in that case with slices of 24 columns width to have some better statistics (8000 profiles in each slice). Figure 24 shows that in this case there is a clear and systematic variation of the cross talk in space, and hence in time given the sequential spatial scanning.

Table 5 lists the determined original and artificial cross talk values. A known added global cross talk could be determined with an accuracy of $2 \cdot 10^{-4}$, but note that it is added to a temporally varying initial value of the order of 10^{-1} with a rms of $2{\cdot}10^{-2}$ in that case.

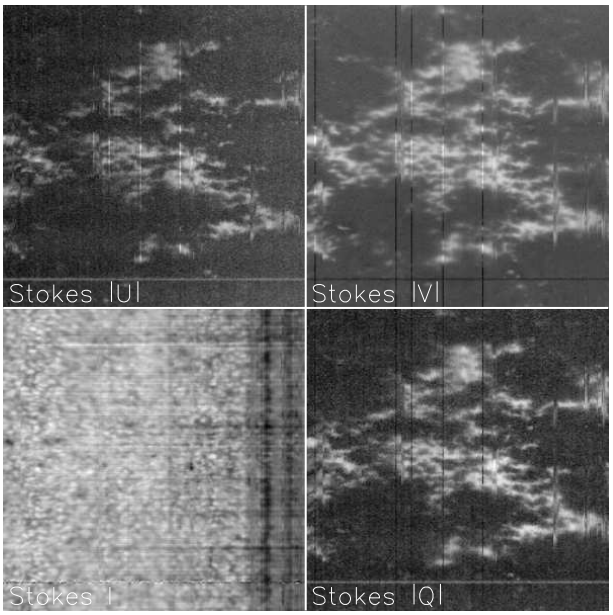

Figure 22: Plage observation near disc center. Stokes Q and U are dominated by residual cross talk from Stokes V and show the same spatial pattern.

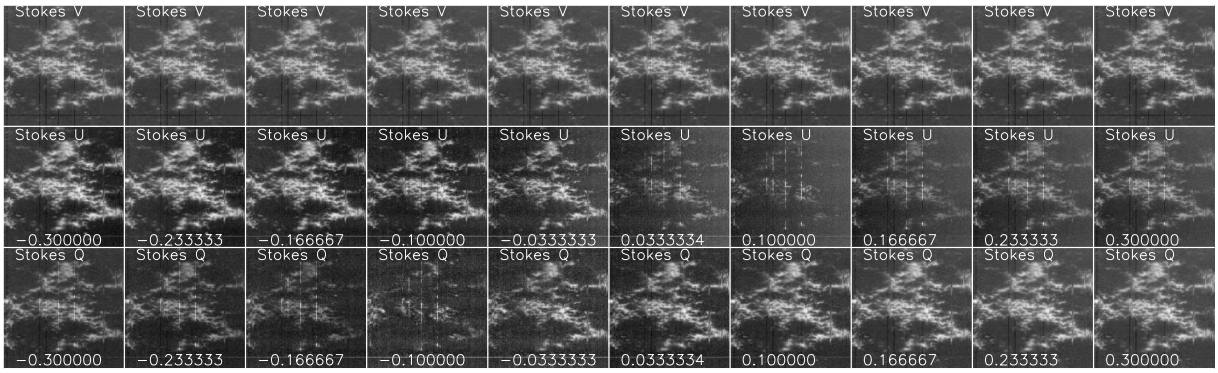

Figure 23: Maps of $|V|$ (top row) and $|Q|$ and $|U|$ at different values of the V→QU cross-talk applied. The cross-talk value is indicated at the bottom of the QU panels. The best correlation values were -0.113 for V→Q and +0.083 for V→U.

9.6 Spectral resolution

To test the effect of the spectral resolution on the result, the initial spectra were re-sized for decreasing spectral resolution. Figure 25 shows and lists the error in the determination of a known cross-talk value as a function of the spectral resolution. At a spectral resolution of about 20,000, the error reaches the percent range, e.g., for Stokes U the measured cross-talk was 0.033 while the true value was 0.020. The sign of the cross-talk was recovered correctly in all cases, and the estimated value was not "far" off even at a resolution of <10,000 (0.0156 instead of 0.0214 in Q, 0.0192 instead of 0.0196 in Stokes U). The plot of the error vs. the resolution shows, however, a clear trend with a strong increase in the error for a spectral resolution below about 40,000.

Table 5: V→QU cross talk values for the plage observations.

	orig	added	known	orig - added	diff
V→Q	-0.11303297	-0.13467183	0.0214	0.0216389	$2 \cdot 10^{-4}$
V→U	0.083047535	0.063624803	0.0196	0.0194227	$2 \cdot 10^{-4}$

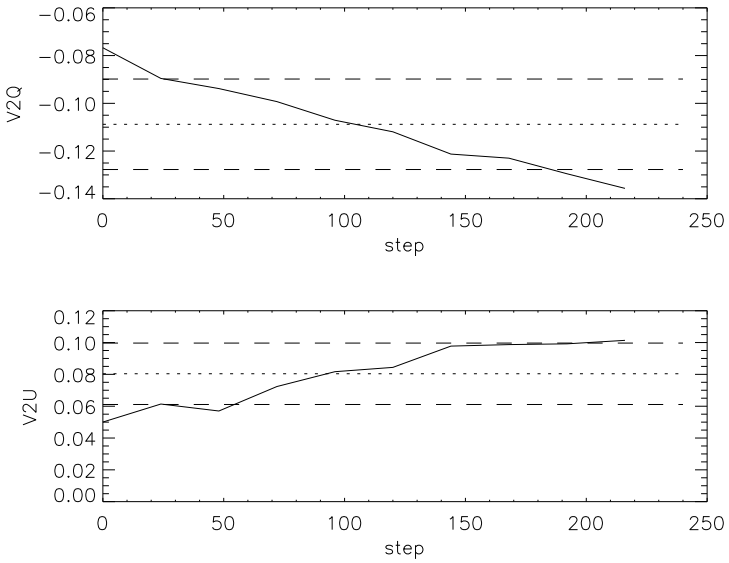

Figure 24: Cross talk V→Q (top) and V→U (bottom) for the plage observation with spatial resolution. Both show a clear spatial, and hence temporal trend.

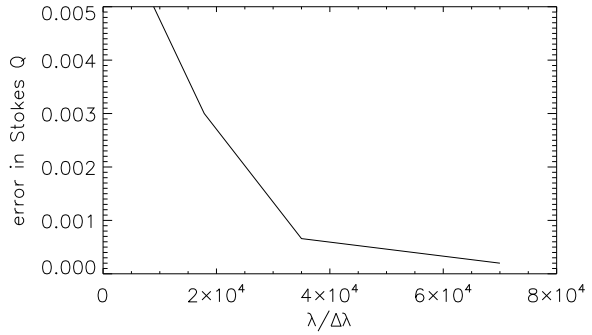

Resolution	Stokes Q	Stokes U
70,000	$2 \cdot 10^{-4}$	$2 \cdot 10^{-4}$
35,700	$6.6 \cdot 10^{-4}$	$2 \cdot 10^{-3}$
17,800	$3 \cdot 10^{-3}$	$1 \cdot 10^{-2}$
8,900	$5 \cdot 10^{-3}$	$4 \cdot 10^{-4}$

Figure 25: Error in the cross-talk determination as a function of spectral resolution.

10 Conclusions: Additional tests

The effects of noise, fringes and the cross-talk amplitude itself are negligible for the accuracy in the determination of a known additional cross talk. The sample size, however, has a strong effect leading to fluctuations of the order of 10^{-2}. The determination of the initial residual cross talk showed such a strong spatial variation, but with primarily a random pattern for the first data set and a clear systematic variation for the 2nd data set.

11 Discussion

The effect of the uncorrected M12 group will be a constant cross talk with no temporal variation on a scale of weeks and very small spatial variation across the field of view that should only be visible for a large FOV of 2.8 arcmin or more. This cross talk will be introduced as first step in the passage through the telescope optics, i.e., prior to, e.g., the creation of interference fringes.

An error in either the telescope model M3-M6 or the modulation matrix M7-detector will in most cases yield a temporal variation in the residual cross talk. For these two components, it does not matter in which of them the actual error is. A "correct" telescope model with an error in the modulation matrix will cause a temporal variation in the residual cross talk in the same way as a "correct" modulation matrix and an incorrect telescope model will do. These two are coupled such thus it will be nearly impossible to locate the error source explicitly.

A separation of the residual cross talk from M3-detector from the cross talk caused by the M12 group will only be possible by concentrating on the primary difference, i.e., the cross talk from the M12 group must be constant in time and cannot depend on the telescope geometry.

12 Recommendations

The following list of recommendations for the determination of cross talk by the M12 group of DKIST seems reasonable:

- A large statistics of 50,000 profiles or more.
- An explicit test for any spatio-temporal variation by using sub-fields of the full FOV. Any systematic low-order variation within 30 min cannot come from the M12 group. For data taken with imaging spectropolarimeters such as the VTF, a single spectral scan should be insensitive to temporal effects. Both for fast imaging spectropolarimetry and slow slit-spectrograph polarimetry multiple data sets at different telescope geometries (> 5) should be used to make sure that about the same constant value is measured at different times/geometries. Any significant temporal variation or large offsets in the cross-talk values between different data sets imply that this cross talk cannot come from the M12 group.
- Using the degree of freedom of the coude table rotation might be helpful. If recording the same solar target at different table angles in a short time (1 hr or less) yields the same cross-talk values, then this supports an origin from the M12 group and no or a low error in the modulation matrix and the telescope model.
- The initial rms noise level of the data should be well below $1{\cdot}10^{-2}$. Solar polarization amplitudes are about 0.3 at maximum, while the predicted cross talk from the M12 group is between $2–8{\cdot}10^{-2}$. That implies a measurement of significant signals of $0.6–2.4{\cdot}10^{-2}$ which implies an rms noise of $0.2–0.8{\cdot}10^{-2}$ for a valid 3-σ detection threshold of the cross talk for the strongest intrinsic solar signal level.
- Spectral resolution can be comparably low with $R = 50,000 - 100,000$.
- Selection of the solar target is critical. The main determination for the M12 group will be the value of the V→U cross talk. Active regions, plage or photospheric network regions close to disc center are the preferred targets to guarantee a large solar circular polarization amplitude.

	true	measured	$V \rightarrow QU$
50 G			
C(V,Q)	0.5421	0.5424	$6.5 \cdot 10^{-5}$
C(V,U)	0.6047	0.6057	-0.00035
100 G			
C(V,Q)	0.5371	0.5378	-0.00011
C(V,U)	0.5804	0.5813	-0.00017
200 G			
C(V,Q)	0.5099	0.5106	-0.00011
C(V,U)	0.5304	0.5311	-0.00015

Table 6: Minimal true and measured correlation value (1st and 2nd column) and cross-talk coefficient of minimal correlation.

- Any of the methods can retrieve known added global cross talk with an accuracy at the 10^{-4} level.

13 Appendix

13.1 Cross talk in MHD simulations

To test the assumption that the intrinsic spatial patterns of Stokes $|QUV|$ lead to minimal correlation in the absence of cross talk, three magneto-hydrodynamic (MHD) quiet Sun simulations were used (see Beck et al. 2017). The MHD runs had an average initial field strength of 50, 100 and 200 G, respectively. The synthetic spectra of the MHD runs for the two Fe I lines at 630.15 and 630.25 nm were used to calculate the maps of wavelength-integrated unsigned $|QUV|$ amplitudes according to Eq. (2). The maps from the original simulation spectra were correlated without and with additional artificial cross talk. Figure 26 and Table 6 demonstrate that minimal correlation between Stokes V and Q and U is reached in the absence of cross talk, i.e., a minimal correlation indicates zero cross talk to the numerical accuracy of the procedure. Note that the correlation values themselves do not reach zero because, e.g., the granulation pattern is to some extent present in all Stokes $|QUV|$ maps.

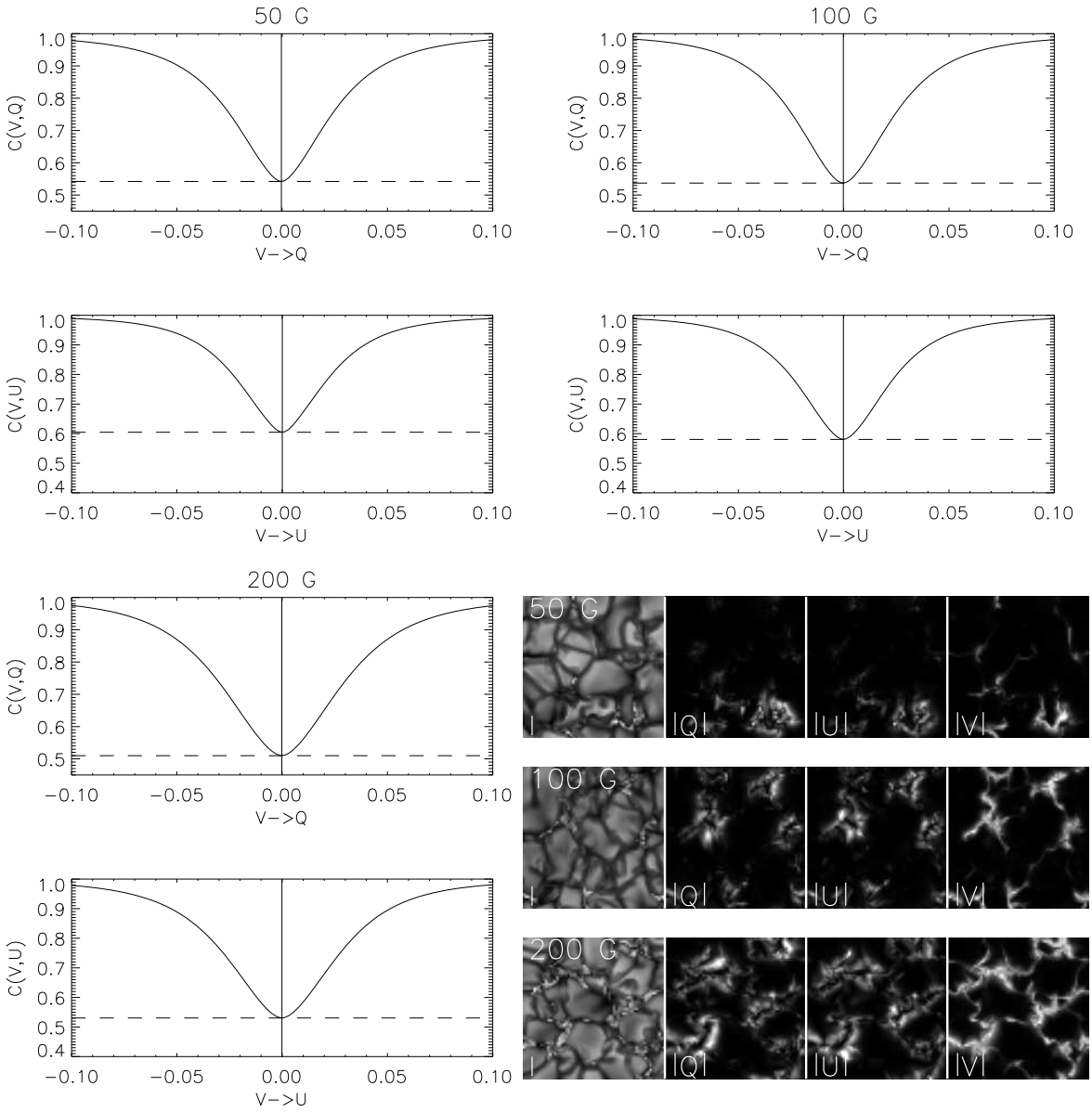

Figure 26: Correlation of Stokes V and Q and U maps at different crosstalk values for MHD simulations with 50 (top left), 100 (top right), and 200 G (bottom right). The dashed lines indicate the correlation value of the original spectra, the vertical solid lines the location with minimal correlation value. Bottom right: maps of IQUV (left to right) from the cross-talk-free simulation spectra. Top to bottom: 50, 100 and 200 G.